



# Macrocerebellum: Volumetric and Diffusion Tensor Imaging Analysis

## *Makroserebellum: Hacimsel ve Diffüzyon Tensor Analizi*

Izlem IZBUDAK<sup>1</sup>, Niyazi ACER<sup>2</sup>, Andrea PORETTI<sup>3</sup>, Kazim GUMUS<sup>4</sup>, Gokmen ZARARSIZ<sup>5</sup>

<sup>1</sup>The Johns Hopkins Hospital, School of Medicine, The Russell H. Morgan Department of Radiology and Radiological Science, Division of Neuroradiology, Section of Pediatric Neuroradiology, Baltimore, USA

<sup>2</sup>Erciyes University, School of Medicine, Department of Anatomy, Kayseri, Turkey

<sup>3</sup>The Johns Hopkins University, School of Medicine, The Russell H. Morgan Department of Radiology and Radiological Science, Division of Pediatric Radiology, Section of Pediatric Neuroradiology, Baltimore, USA

<sup>4</sup>Erciyes University, School of Medicine, Department of Biophysics, Kayseri, Turkey

<sup>5</sup>Erciyes University, School of Medicine, Department of Biostatistics, Kayseri, Turkey

Corresponding Author: Izlem IZBUDAK / E-mail: iizbuda1@jhmi.edu

### ABSTRACT

Macrocerebellum is a rare entity characterized by an enlarged cerebellum. We describe a case of a 48-month-old child with macrocerebellum. We performed serial volumetric analysis [total brain volume (TBV) and cerebellar volume] over a period of 4 years. We analyzed the white matter microstructure in the cerebellum using diffusion tensor imaging (DTI). In our patient, we found higher fractional anisotropy (FA) and lower mean diffusivity (MD) in the cerebellar white matter compared to age-matched controls. Our results may represent accelerated myelination secondary to the abnormal cerebellar development.

**KEYWORDS:** Macrocerebellum, Cerebellar volume, Total brain volume, Volume ratio, Diffusion tensor imaging

### ÖZ

Nadir görülen bir hastalık olan makroserebellum, isminden de kolayca anlaşılacağı gibi serebellumun anormal bir şekilde büyük olması anlamına gelir. Bu çalışmada 48 aylık bir makroserebellum olgusu sunulmaktadır. Toplam beyin hacmi ve serebellum hacmi 4 yıllık bir periyotta 3 boyutlu manyetik rezonans görüntüleme (MRG) ile ölçülerek zaman içerisinde değişimi incelenmiştir. Hastanın MR görüntüleri üzerinde aynı zamanda atlas temelli diffüzyon tensör görüntüleme (DTG) analizi yapılmış, beyinciğin beyaz cevherinde fraksiyonel anizotropi (FA) ile ortalama diffüzyon (OD) değerleri hesaplanmış ve kontrollerle karşılaştırıldığında kontrol grubuna göre FA değerinin daha yüksek, OD değerinin daha düşük olması nedeni ile bu durumun serebellum gelişiminin anormalliğinden dolayı hızlı miyelinizasyona işaret edebileceği düşünülmüştür.

**ANAHTAR SÖZCÜKLER:** Makroserebellum, Serebellar hacim, Toplam beyin hacmi, Hacim oranı, Difüzyon tensor görüntüleme

### INTRODUCTION

Macrocerebellum is a rare finding characterized by an abnormally large cerebellum (14). The diagnosis is based on the neuroimaging findings including enlargement of the cerebellum in a normal sized posterior fossa. The cerebellar enlargement involves particularly the cerebellar hemispheres, which expand into adjacent anatomic regions by wrapping around the brainstem and herniating upward or downward. A macrocerebellum may occur within the neuroimaging spectrum of well-defined diseases or syndromes including Sotos syndrome, Costello syndrome, Williams syndrome, macrocephaly-capillary malformation syndrome, Alexander disease, fucosidosis, mucopolysaccharidoses or Lhermitte-Duclos disease (2, 15). Additionally, few patients with an isolated (non-syndromal) macrocerebellum have been reported (3, 14, 16).

The pathogenesis of macrocerebellum remains unknown. Qualitative MR evaluation suggested that thickening of the cortical gray matter of the cerebellar hemispheres may be responsible for the macrocerebellum in non-syndromal patients. Poretti et al. hypothesized that macrocerebellum

may not be a nosological entity, but instead represents the structural manifestation of a biological disturbance in the cerebellar development that is common to heterogenous disorders and may occur at different stages of the cerebellar development (16). Accordingly, in contrast to diseases such as fucosidosis, Costello syndrome or Alexander disease, in non-syndromal patients macrocerebellum does not represent a progressive cerebellar enlargement.

Here we report on serial volumetric studies in a child with a non-syndromal macrocerebellum. Additionally, we analyzed the microstructure of the cerebellar white matter using diffusion tensor imaging (DTI).

### CASE REPORT

#### *Patient*

Our patient is a 4-year-old boy who presented for the first time at the age of 6 months because of hydrocephalus. Subsequently, a ventriculo-peritoneal shunt was placed and several magnetic resonance (MR) follow-ups have been performed.

### Conventional MRI and DTI

All MRI studies were acquired on a 1.5-T clinical MR scanner (Avanto, Siemens, Erlangen, Germany) using a standard 8-channel head coil. The standard departmental protocol includes a 3D-T1-weighted image (TR 1130 msec, TE 3.99 msec, slice thickness 1.0 mm, field-of-view FOV 240x240 mm, matrix size 192x192), and axial T2-weighted image and fluid attenuation inversion recovery (FLAIR) sequence and a single-shot spin echo, echo planar axial DTI sequence with diffusion gradients along 20 non-collinear directions. An effective high b-value of 1000 sec/mm<sup>2</sup> was used for each of the 20 diffusion-encoding directions. We performed an additional measurement without diffusion weighting (b = 0 sec/mm<sup>2</sup>). For the acquisition of the DTI data, the following parameters were used: TR 7100 msec, TE 84 msec, slice thickness 2.5 mm, field-of-view 240 × 240 mm, and matrix size 192 × 192. Parallel imaging iPAT factor 2 (Siemens) with GRAPPA (generalized auto-calibrating partial parallel acquisition reconstruction) was used. The acquisition was repeated twice to enhance the signal-to-noise ratio.

### Volumetric Analysis

MR images were saved using ImageJ software (<http://rsb.info.nih.gov/ij>) as two files with extensions ".hdr" and ".img". The MR images were opened and stacked using ImageJ. (Figure 1A). Before calculating the total brain volume (TBV) for the given Analyze image, the skull was stripped off the brain (11). The brain extraction was performed using MRICro (<http://www.mccauslandcenter.sc.edu/mricro/mricro/index.html>) Brain Extraction Tool (BET) (Figure 1B). Volume estimation was performed with the EasyMeasure program ([www.liv.ac.uk/mariarc](http://www.liv.ac.uk/mariarc)) (4,12). This software summated automatically the area of each slice and the TBV was calculated using the Cavalieri principle (12). An unbiased estimation of the volume was obtained as the sum of the estimated areas of the structure transects on consecutive systematic sections multiplied by the distance between sections. Once the point counting grid was placed, the points falling within the brain section were automatically counted. The EasyMeasure program allows the user to determine contrast, select true threshold value to estimate counting automatically (4, 5).

Since 1 mm was used for both the slice thickness and the distance between two test points of the grid, the TBV could be easily estimated. A 1 × 1 × 1 mm grid was chosen, indicating a grid point spacing of 1 mm in the plane of the image and through the depth of the volume (Figure 1C). The volume fraction of the cerebellum over the total brain was calculated by means of volume fraction approach (7, 13).

Coefficient of error (CE) and confidence interval (CI) calculations were performed according to García-Fiñana et al. (9, 10). In this study, the own codes have been written and the CE and CI values have been predicted using R 3.0.1 software ([www.r-project.org](http://www.r-project.org)). Related codes can be found in Suppl. material.

### DTI Post-Processing

All DTI datasets were processed offline using DTIStudio, ROEditor and DiffeoMap software (available at [www.MRIStudio.org](http://www.MRIStudio.org)). After correcting for eddy currents and motion artifacts, all images were coregistered to one another using a 12-mode affine transformation of Automated Image Registration (AIR). Subsequently, the following maps were generated: fractional anisotropy (FA), vector, color-coded fractional anisotropy, and trace of diffusion. After skull-stripping, the images were subsequently normalized to the MNI coordinates using a nine-parameter affine linear transformation of AIR. For this transformation, b<sub>0</sub> images were used for both the subject data and the JHU-MNI "Eve" template. Subsequently, a non-linear transformation using a dual-contrast (FA and trace of diffusion) large deformation diffeomorphic metric mapping (LDDMM) was applied. Atlas-based analysis was finally performed using a white matter parcellation map (WMPM) of the JHU-MNI "Eve" template and the brain was parcellated into 159 anatomical regions including both gray and white matter. Because of the reciprocal nature of both linear and non-linear transformation, the transformation results was used to warp the WMPM to the original DTI data, thus automatically segmenting each brain into the 159 subregions (Figure 2). FA and mean diffusivity (MD=Trace of diffusion/3) have been calculated for middle cerebellar peduncle (MCP). Fiber tractography (FT) reconstruction of the MCP was performed using DTIStudio software. We applied the FACT algorithm, a FA threshold of 0.25 and a deflection angle of 40°. FT of the MCP was performed by positioning seed points as previously reported: two seeds points were placed on the parasagittal images where the MCP were greatest in volume and two additional seed points were placed laterally to the lateral pontine tegmentum on both sides (Figure 3) (17, 18). Color-coded FA maps were used to guide placement of the seed points.

### Results

For our patient, 5 conventional MRI studies were acquired at the age of 6 months, 1 year, 2 years, 3 years and 4 years. A qualitative retrospective evaluation of these MR studies showed that a macrocerebellum was already present at the age of 6 months.

Quantitative volumetric analysis in our patient revealed a cerebellar volume of 85.4, 106.4, 133.8, 147.4 and 161.0 cm<sup>3</sup> at the five different ages (Figure 4B). At the same ages, the TBV was 1142.5, 1044.3, 1254.6, 1461.3 and 1652.4 cm<sup>3</sup>, respectively (Figure 4A). For each measurement, we calculated the ratio between the cerebellar volume and the TBV. At the five different ages, this ratio was 7.5%, 10.2%, 10.7%, 10.1% and 9.7%, respectively (Figure 4C). We compared each single volumetric measurement of our patient with age-matched controls. Five age-matched controls for each MRI study of our patient were selected from our pediatric MR database using following criteria: normal brain anatomy, absence of neurological disorder and availability of 3D-T1-

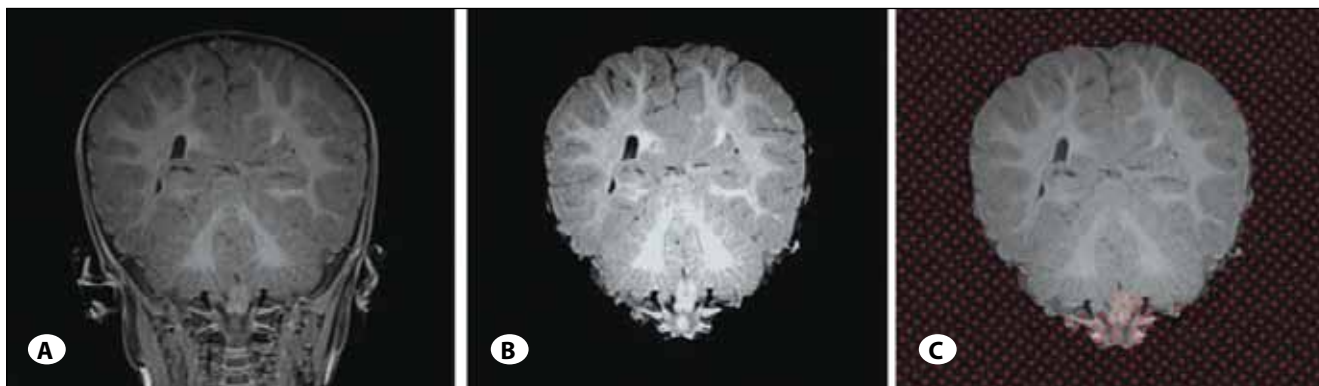


**Figure 1:** Original image (A), BET using MRICro (B), a point-counting grid superimposed using Easymeasure (C).

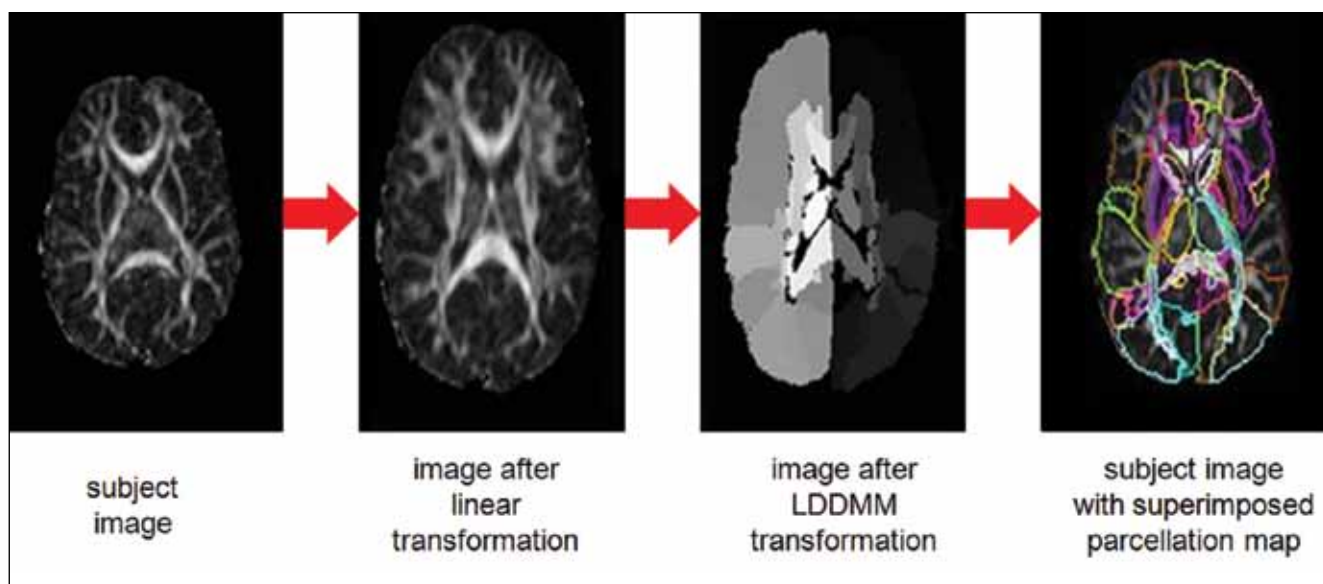


**Figure 2:** Normalization procedures of the DTI maps. Subject images are normalized to an atlas using a linear (affine) transform, followed by a non-linear (LDDMM) transform respectively. These figures show parcellation of subject brain images into 159 subregions.

weighted images. For the 5 control groups, the cerebellar volume (mean±standard deviation) was 69.1±9.7, 101.2±7.0, 125.8±21.6, 134.5±21.5 and 134.1±21.5 cm<sup>3</sup> and the TBV was 854.0±93.3, 1099.4±55.0, 1326.6±204.8, 1365.2±71.4, 1371.8±185.6 cm<sup>3</sup>. This resulted in a ratio between cerebellar volume and TBV of 8.1%, 9.2%, 9.4%, 9.9% and 9.8% for the 5 controls groups, respectively (Figure 4).

For the cerebellar white matter quantitative analysis we used DT images of our case at 24 months of age and DTI of one control subject at the same age. In the right and left MCP, DTI analysis revealed FA values of 0.26 and 0.27 and MD values of 0.906 x 10<sup>-3</sup> and 0.871 x 10<sup>-3</sup> mm<sup>2</sup>/s, respectively. The same DTI post-processing in age-matched control revealed FA values of 0.21 and MD values of 0.943 x 10<sup>-3</sup>mm<sup>2</sup>/s in both MCP's, respectively.

**DISCUSSION**

The cerebellum develops over a long period of time extending from the very early embryonic period until the first years of life.

After the neural tube is formed, neurons of the mid-hindbrain are generated in the neuroepithelium that lines the walls of the fourth ventricle (6). The cerebellum develops from the dorsal anterior hindbrain (rhombomere 1) and the majority of its neurons are generated in two distinct germinal matrices: the adjacent dorsal ventricular zone, which generates the Purkinje cells and the dorsal and rostral portions of the rhombic lip, which generates neuronal precursors of the granule cells (6). After generation in the rhombic lip, granule cells migrate tangentially and form a transient external granular layer on the outside of the developing cerebellar hemispheres. In the external granular layer, the immature granule cells undergo many cycles of mitosis and differentiate into granule neurons, which migrate inwards to form the internal granular layer in the cerebellar hemispheres. This process continues into the first postnatal years and causes a marked increase in the size of the cerebellum in the first 2 years of life (19). In 50 healthy children, Wu et al. performed quantitative volumetric analysis of the cerebellar growth from birth to the adolescence and

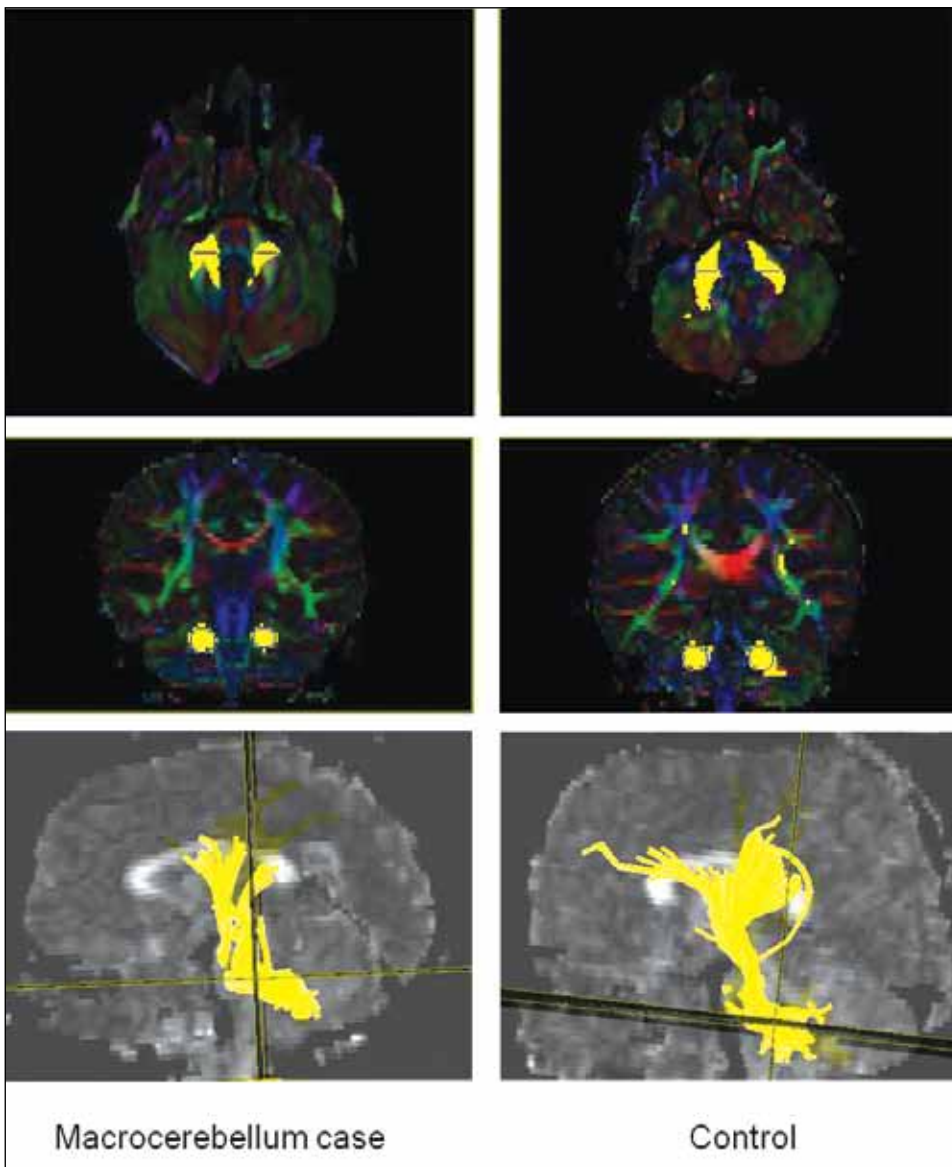


**Figure 3:** Fiber tracking of the MCP. Axial and coronal color-coded maps showing the MCP in yellow color. Two ROIs were placed at the sagittal image.

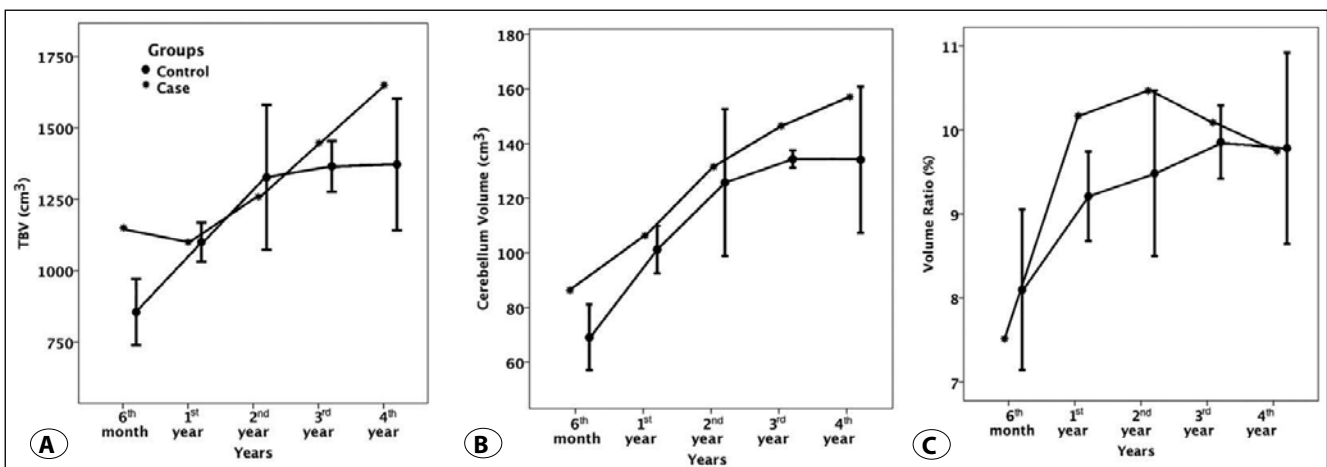


**Figure 4:** The graphs demonstrate total brain volume (A), cerebellum volume (B) and volume ratio (C) during four years in our patient versus controls with approximate 95% confidence intervals.

found that the growth of the unmyelinated cerebellum (including the cerebellar gray matter) is mainly responsible for the cerebellar growth within the first postnatal years (19).

In our study, the longitudinal volumetric measurements show that the cerebellar growth in the non-syndromal macrocerbellum patient is high in the first three years of age, while it decreases later on. At the age of 4 years, the ratio between cerebellar volume and TBV is the same for patient and controls. This finding matches the hypothesis by Poretti et al. that the large cerebellar size in non-syndromal macrocerbellum patients is not caused by a progressive cerebellar enlargement, but disturbances that disrupt the cerebellar development at different stages (16).

The qualitative neuroimaging evaluation of five children with non-syndromal macrocerbellum by Poretti et al. revealed that the large cerebellar size was caused by thickening of the cerebellar gray matter within the cerebellar hemispheres (16). They hypothesized that macrocerbellum may be caused by an abnormal (increased) growth of the cerebellar granule cells. As discussed above, granule cells play a key role for the physiological increase in cerebellar size until the age of 2 years. The highest increase in cerebellar size in our patient occurred during this period of time. This time overlap supports the potential role of the granule cells in the pathomechanism of non-syndromal macrocerbellum.

The white matter developmental process is characterized by structural changes including an increase in myelin and white matter packing and decrease in water content (8). These changes cause a reduction of movements of intracellular water, which are restricted perpendicular to the length of the axon rather than parallel to it. Using DTI, these changes may be quantified as increase in FA and decrease in MD. In our patient, DTI analysis revealed higher FA and lower MD in the MCP compared to an age-matched control. Although the differences in DTI metrics are rather small, they may suggest a higher stage of white matter maturation for the patient compared to the control. It is arguable that the cerebellar development is increased not only in terms of size, but also of white matter maturation in non-syndromal macrocerbellum. DTI analysis of the cerebellar white matter in further patients with non-syndromal macrocerbellum is needed to confirm this hypothesis.

We are aware of several limitations in this study: we were able to include only one patient with non-syndromal macrocerbellum, the DTI analysis included only one age-matched control, the small sample does not allow statistical analysis, and no clinical data are available for our patient.

In summary, our longitudinal volumetric analysis in one patient with non-syndromal macrocerbellum supports the hypothesis of Poretti et al that macrocerbellum may be caused by an abnormal (increased) development of cerebellar granule cells until the end of the first postnatal years. Additionally, DTI analysis may suggest that in macrocerbellum the abnormal cerebellar development may not be limited only to the size, but may also affect the white matter microstructure.

## REFERENCES

1. Acer N, Turgut M: Anatomy of cerebellum. In: Turgut M (ed), *Cerebellar Mutism: From Definition to Treatment*, Nova Science Publishers Inc 2012:12-20
2. Alqahtani E, Huisman TAGM, Boltshauser E, Scheer I, Güngör T, Tekes A, Maegawa GH, Poretti A: Mucopolysaccharidoses type I and II: New neuroimaging findings in the cerebellum. *Eur J Paediatr Neurol* 18(2):211-217, 2014
3. Bodensteiner JB, Schaefer GB, Keller GM, Thompson JN, Bowen MK: Macrocerbellum: Neuroimaging and clinical features of a newly recognized condition. *J Child Neurol* 12:365-368, 1997
4. Denby CE, Vann SD, Tsivilis D, Aggleton JP, Montaldi D, Roberts N, Mayes, AR: The frequency and extent of mammillary body atrophy associated with surgical removal of a colloid cyst. *AJNR Am J Neuroradiol* 30:736-743, 2009
5. Doherty CP, Fitzsimons M, Holohan T, Hasssbo BM, Farrell M, Meredith GE, Staunton H: Accuracy and validity of stereology as a quantitative method for assessment of human temporal lobe volumes acquired by magnetic resonance imaging. *Magn Reson Imaging* 8:1017-1025, 2000
6. Doherty D, Millen KJ, Barkovich AJ: Midbrain and hindbrain malformations: Advances in clinical diagnosis, imaging, and genetics. *Lancet Neurol* 12:381-393, 2013
7. Ekinci N, Acer N, Akkaya A: Volumetric evaluation of the relations among the cerebrum, cerebellum and brain stem in young subjects: A combination of stereology and magnetic resonance imaging. *Surg Radiol Anat* 30:489-494, 2008
8. Faria AV, Zhang J, Oishi K, Li X, Jian H, Akhter K, Hermoye L, Lee SK, Hoon A, Stashinko E, Miller MI, van Zijl PC, Mori S: Atlas-based analysis of neurodevelopment from infancy to adult hood using diffusion tensor imaging and applications for automated abnormality detection. *Neuroimage* 52:415-428, 2010
9. García-Fiñana M, Cruz-Orive LM, Mackay CE, Pakkenberg B, Roberts N: Comparison of MR imaging against physical sectioning to estimate the volume of human cerebral compartments. *Neuroimage* 18:505-516, 2003
10. García-Fiñana M, Keller SS, Roberts N: Confidence intervals for the volume of brain structures in Cavalieri sampling with local errors. *J Neurosci Methods* 179:71-77, 2003
11. Karsch K, Grinstead B, He Q, Duan Y: Web Based Brain Volume Calculation for Magnetic Resonance Images. 30th Annual International IEEE EMBS Conference, Vancouver, British Columbia, Canada, August 20-24, 2008
12. Keller SS, Roberts N: Measurement of brain volume using MRI: Software, techniques, choices and prerequisites. *J Anthropological Sci* 87:127-151, 2009
13. Nisari M, Ertekin T, Ozcelik O, Cinar S, Doğanay S, Acer N: Stereological evaluation of the volume and volume fraction of newborns' brain compartment and brain in magnetic resonance images. *Surg Radiol Anat* 34:825-832, 2012
14. Pichiecchio A, Di Perri C, Arnoldi S, Berardinelli A, Branca V, Balottin U, Bastianello S: Cerebellum enlargement and corpus callosum agenesis: A longitudinal case report. *J Child Neurol* 26:756-760, 2011

15. Poretti A, Boltshauser E. Macrocerbellum. In: Boltshauser E, Schmahmann JD, (eds). *Cerebellar disorders in children*. London: Mac Keith Press, 2012:192–193
16. Poretti A, Mall V, Smitka M, Grunt S, Risen S, Toelle SP, Benson JE, Yoshida S, Jung NH, Tinschert S, Neuhann TM, Rauch A, Steinlin M, Meoded A, Huisman TA, Boltshauser E: Macrocerbellum: Significance and pathogenic considerations. *Cerebellum* 11:1026-1036, 2012
17. Salamon N, Sicotte N, Drain A, Frew A, Alger JR, Jen J, Perlman S, Salamon G: White matter fiber tractography and color mapping of the normal human cerebellum with diffusion tensor imaging. *J Neuroradiol* 34:115–128, 2007
18. Wakana S, Jiang H, Nagae-Poetscher LM, vanZijl PC, Mori S: Fiber tract-based atlas of human white matter anatomy. *Radiology* 230:77–87, 2004
19. Wu KH, Chen CY, Shen EY: The cerebellar development in chinese children-a study by voxel-based volume measurement of reconstructed 3D MRI scan. *Pediatr Res* 69:80-83, 2011